Biochem. J. (2014) **458**, 225–237 (Printed in Great Britain) doi:10.1042/BJ20130792

A purine nucleoside phosphorylase in *Solanum tuberosum* L. (potato) with specificity for cytokinins contributes to the duration of tuber endodormancy

Jennifer R. BROMLEY*[1], Barbara J. WARNES*, Christine A. NEWELL*, Jamie C. P. THOMSON*[2], Celia M. JAMES*, Colin G. N. TURNBULL† and David E. HANKE*[3]

*Department of Plant Sciences, University of Cambridge, Downing Street, Cambridge CB2 3EA, U.K.
†Department of Life Sciences, Imperial College London, London SW7 2AZ, U.K.

StCKP1 (*Solanum tuberosum* cytokinin riboside phosphorylase) catalyses the interconversion of the N^9-riboside form of the plant hormone CK (cytokinin), a subset of purines, with its most active free base form. StCKP1 prefers CK to unsubstituted aminopurines. The protein was discovered as a CK-binding activity in extracts of tuberizing potato stolon tips, from which it was isolated by affinity chromatography. The N-terminal amino acid sequence matched the translation product of a set of ESTs, enabling a complete mRNA sequence to be obtained by RACE-PCR. The predicted polypeptide includes a cleavable signal peptide and motifs for purine nucleoside phosphorylase activity. The expressed protein was assayed for purine nucleoside phosphorylase activity against CKs and adenine/adenosine. Isopentenyladenine, *trans*-zeatin, dihydrozeatin and adenine were converted into ribosides in the presence of ribose 1-phosphate. In the opposite direction, isopentenyladenosine, *trans*-zeatin riboside, dihydrozeatin riboside and adenosine were converted into their free bases in the presence of P_i. StCKP1 had no detectable ribohydrolase activity. Evidence is presented that StCKP1 is active in tubers as a negative regulator of CKs, prolonging endodormancy by a chill-reversible mechanism.

Key words: cytokinin, endodormancy, interconversion, plant hormone, purine riboside phosphorylase, *Solanum tuberosum*.

INTRODUCTION

Naturally occurring CKs (cytokinins) are modified forms of the nucleic acid base Ade (adenine) with plant growth regulating activity. CKs play a role in many aspects of plant growth and development, including cell division, cell enlargement, senescence and differentiation. CK biochemistry resembles that of other purines, with N^9-ribosides and their phosphate esters as universally occurring forms. CKs are synthesized as ribonucleotides and metabolic studies show that the three forms, ribotide, riboside and free base, are interconverted in a dynamic cycle, whereas other derivatives are sequestered metabolic dead ends [1,2]. CKs are effective long-distance signals transported around the plant in the xylem and the phloem. Since the xylem-transported forms are predominantly ribosides [1], but the CK receptors AHK2 (*ARABIDOPSIS* HISTIDINE KINASE 2), AHK3 and AHK4 show a strong preference for the free base [3,4], it follows that the reactions interconverting the transported ribosides and the perceivable free bases (Figure 1) are potential control points.

In *Arabidopsis thaliana* vegetative tissue, the major route for the release of CK free bases from ribotides has been shown to be via a CK riboside-5′-monophosphate phosphoribohydrolase reaction catalysed by LOG (LONELY GUY) proteins in the cytosol. When sets of *LOG* genes were up-regulated, responsiveness to CK was increased, evidence that release of the free base form by LOGs controls many responses to CK [5].

The only known alternatives to LOG for generating the active free base forms of CKs are enzymes of the Ade salvage pathway which primarily interconvert the riboside, ribotide and free base forms of Ade, but which will also accept CK substrates. The same enzymes that process the intermediary metabolites Ado (adenosine) and its 5′-phosphate esters may also catalyse the equivalent reactions for CK riboside and ribotides. For some reactions, plants have versions of these enzymes specialized for processing CKs [6,7].

5′-nucleotidases catalyse the release of ribosides from ribotides. Two 5′-nucleotidases from wheat germ had similar low micromolar K_m values for both AMP and iPR (isopentenyladenosine) 5′-monophosphate [8]. From the ribosides, there are two routes to the free base: via Ado kinase [9] and LOG in sequence, or alternatively by cleavage of the N^9-glycosidic linkage. The route via Ado kinase is self-evidently not an alternative to LOG, which leaves two enzyme activities reported for plants: purine riboside ribohydrolase and purine riboside phosphorylase. The ribohydrolase reaction on the riboside irreversibly releases free base, but a phosphorylase could catalyse the reaction in either direction. There are numerous reports of Ado ribonucleosidase activity from plants, but with one exception the enzymes prefer substrates other than CKs, and their K_m values for CK ribosides are unphysiologically high [10–12]. Only a wheat germ nucleosidase [13] showed activity against iPR comparable with that for Ado, with a low apparent K_m value of 2.4 μM for iPR. Purine nucleoside phosphorylase, on the other hand, is rarely reported for plants, although it is widespread in animals and micro-organisms. Chen and Petschow [14] characterized an Ado phosphorylase from wheat germ with a K_m value for Ade of 32 μM. iP (isopentenyladenine) was also a substrate, but with an even higher

Abbreviations: Ade, adenine; Ado, adenosine; AHK2, *ARABIDOPSIS* HISTIDINE KINASE 2; BT, before tuberization; CaMV, cauliflower mosaic virus; CDS, coding DNA sequence; CK, cytokinin; DZ, dihydrozeatin; DZR, dihydrozeatin riboside; EPI, enhanced product ion; FM, fresh mass; iP, isopentenyladenine; iPR, isopentenyladenosine; IT, incipient tuberization; LOG, LONELY GUY; MRM, multiple reaction monitoring; MWCO, molecular-mass cut-off; PVX, potato virus X; R1-P, ribose 1-phosphate; RP, reverse-phase; RT, reverse transcription; StCKP1, *Solanum tuberosum* cytokinin riboside phosphorylase; VIGS, virus-induced gene silencing; Z, *trans*-zeatin; ZR, *trans*-zeatin riboside.

[1] Current address: Feedstocks Division, Joint BioEnergy Institute, Emeryville, CA 94608, U.S.A., and Physical Biosciences Division, Lawrence Berkeley National Laboratory, Berkeley, CA 94720, U.S.A.
[2] Current address: Pfizer Inc, Eastern Point Road, Groton, CT 06340, U.S.A.
[3] To whom correspondence should be addressed (email deh1000@cam.ac.uk).

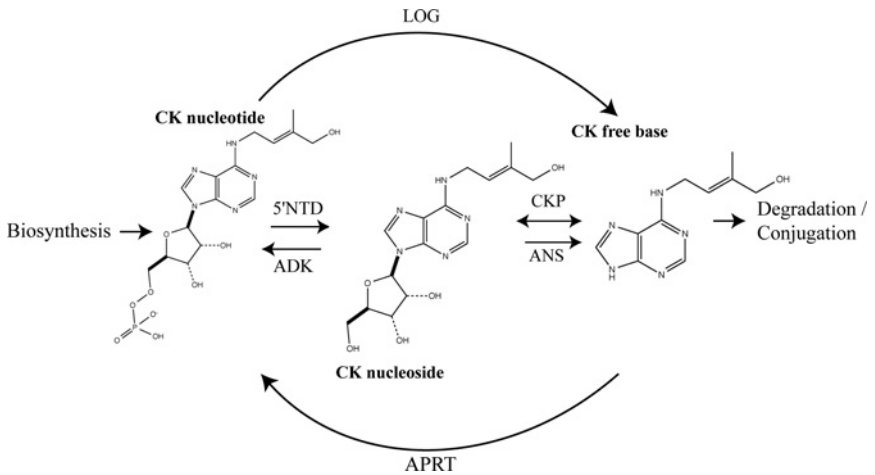

Figure 1 Schematic model for the interconversion of CKs

The pathway is illustrated using *trans*-zeatin-type CKs, but is equally applicable to the interconversion of *cis*-zeatin-, iP- and DZ-type CKs. ADK, Ado kinase; ANS, Ado nucleosidase; APRT, Ado phosphoribosyltransferase; 5′NTD, 5′-nucleotidase.

K_m value of 57 μM, far higher than physiologically active and mean tissue concentrations of CKs [15].

As an experimental system, potato has a number of advantages for the study of CKs. First, it is one of few plants from which sufficient shoot apices, a prime target organ for CKs, for chemical analysis can be obtained without dissection, in the form of stolon tips and tuber buds. Secondly, CKs regulate progress through the predominant asexual life cycle of the potato, in which vegetative growth in favourable conditions alternates with a period of dormancy as a stem tuber. By their effects on shoot apices CKs influence the entry to [16,17], and control the departure from [18,19], the tuber stage. Individuals are locked into the tuber stage by endodormancy of tuber buds, the form taken by the shoot apical meristems in the tuber stage. Endodormancy is an internally imposed state of zero growth and minimal metabolism with a characteristic duration that is typically shortened in response to chill treatment: a period of exposure to temperatures near but not below freezing, signifying the early stages of a cold season. Ending endodormancy in response to this signal allows buds of temperate perennials to resume growth whenever the cold season ends [20]. We have previously shown that the exit from endodormancy in potato tubers is the result of an increase in both the CK content of tuber buds and in the sensitivity of tuber buds to activation by CK, and that chilling shortens dormancy by accelerating both of these increases [18,21]. The extra dormancy associated with unchilled tubers is referred to in the present paper as the chill-responsive component of endodormancy.

We report a nucleoside phosphorylase superfamily protein, isolated from potato (*Solanum tuberosum* L.) shoot apices, which interconverts CK ribosides and free bases in preference to the interconversion of Ado and Ade. We provide evidence that this newly discovered CK riboside phosphorylase specifically acts to extend the chill-responsive component of endodormancy. CKs function to reactivate meristematic activity in tuber buds and can be thought of as negative regulators of dormancy, from which we reason that this CK-binding CK-modifying enzyme prolongs the duration of endodormancy by lowering CK activity. Shortening of endodormancy in response to chill treatment would therefore involve eliminating the down-regulation of CKs by CK riboside phosphorylase.

EXPERIMENTAL

Plant material

Plants of both non-transformed control *S. tuberosum* L. cv. Desiree and transformed lines were maintained in aseptic culture on solid MS30 medium [1 × Murashige and Skoog medium including modified vitamins and 3 % (w/v) sucrose, pH 5.8, plus 0.8 % phytoagar supplemented with 50 μg/ml kanamycin if applicable] in a growth room (21 °C, 16 h light/8 h dark, 200 μmol·m^{-2}·s^{-1} photosynthetically active radiation, 65 % humidity) before transfer to soil (Levington M3, Scotts; pot diameter 40 cm) in the same controlled environment. Soil moisture was maintained at a minimum of 45 %. Tubers were harvested when leaves began to senesce.

S. tuberosum L. cv. Majestic was grown at the Cambridge University Botanic Garden. Shortly after all shoots had completed senescence, tubers were dug out of the ground and washed. A total of 30 tubers >4 cm and <10 cm diameter and free from visible blemish were placed in the bottom of a large paper sack, tying the sacks to exclude light, and incubated at approximately 15 °C. Tubers sprouted after 3 months, developing long branched stems: 'stolons'. Stolon tips in vegetative growth were collected after 6 months in bags ('before tuberization': BT stage), and again after 9 months, just before the stolon tips swelled in the first visible manifestation of tuberization ('incipient tuberization': IT stage), achieved by selecting non-tuberizing stolon tips from tubers, some of whose stolons had begun to tuberize. Tips (0.5 cm–1 cm in length) were cut, immediately flash-frozen in liquid nitrogen and stored at − 80 °C.

Protein extraction

Tissues were ground in liquid nitrogen and mixed with 0.1 g of polyvinylpolypyrrolidone per g of FM (fresh mass) before transferring to 3 volumes of pre-chilled extraction buffer containing 50 mM Tris/HCl, 1 mM EDTA, 5 mM $MgCl_2$, 4 mM glutathione, 1 mM PMSF and 100 mM sodium ascorbate, pH 7.4. Thawed slurry was filtered through muslin and the filtrate was centrifuged at 1000 ***g*** for 1 h. The supernatant was removed and centrifuged for a further 1 h at 32 000 ***g***. Protein was precipitated by the addition of solid ammonium sulfate. The supernatant was

brought to 50 % saturation with ammonium sulfate, stirred for 100 min on ice then centrifuged at 18 000 ***g*** for 25 min. The supernatant was brought to 75 % saturation with ammonium sulfate before stirring and centrifuging as above. The pellets were gently resuspended in 1 ml of assay buffer (5 mM $MgCl_2$ and 50 mM Tris/HCl, pH 7.2) and combined before desalting on a 9 ml bed volume of pre-equilibrated Sephadex G-25.

Equilibrium dialysis

Teflon sample cells in two halves each with a working volume of 0.7–1 ml (Dianorm Geräte) were used with a dialysis membrane of 5000 Da MWCO (molecular-mass cut-off). Extracted protein (1 ml) in assay buffer was loaded into one half of the cell and the other half contained 1 ml of ZR-[^{3}H]diol, a tritiated derivative of ZR (*trans*-zeatin riboside), as tracer in assay buffer, specific activity 174 MBq·μmol^{-1}. ZR-[^{3}H]diol is periodate-oxidized ZR reduced with tritiated borohydride following the method of Turnbull and Hanke [21], and was used for binding studies because the intact zeatin moiety provided comparable affinity with that of Z (*trans*-zeatin) and ZR without potential complications arising from conversion by enzyme activity. The cells were sealed and rotated at 0.17 Hz for 14 h at 4 °C. Following incubation, samples from each half cell were collected and 0.9 ml was added to 4 ml of Optiphase Hi-Safe 3 liquid scintillation fluid (PerkinElmer) for radioactivity determination. The half-cell initially containing the protein extract ultimately contained the protein, bound tracer and half of the unbound tracer, the latter being evenly distributed between the two halves of the cell.

For tissue specificity studies, protein was prepared from young leaves and storage pith of maturing tubers, both collected at the Botanic Garden, and stolon tips after 6 and 9 months in storage (BT and IT stages). Samples of protein diluted to different extents with assay buffer were equilibrium dialysed against the same volume of 1.41 nM ZR-[^{3}H]diol in assay buffer to determine the binding activity.

For ligand specificity studies, protein was prepared from stolon tips at the IT stage, pre-incubated at 21 mg·ml^{-1} with 5.2 nM ZR-[^{3}H]diol for 14 h, then equilibrium dialysed against the same volume of assay buffer (control) or a 20 μM solution of a competing ligand in assay buffer. The displacement of ZR-[^{3}H]diol by the competing ligand was calculated as a percentage of the control value for binding activity. For affinity determination, a 25 mg·ml^{-1} solution of IT stage stolon tip protein was dialysed against chemical concentrations of ZR-[^{3}H]diol from 1.4 to 130 nM, and the data were transformed according to Scatchard [22].

Isolation of CK-binding proteins

CK-binding proteins were retained on an avidin–Sepharose column preloaded with a chemical conjugate of CK covalently bonded to biotin. Biotinylated ZR was prepared as follows. After dropwise addition of 10 mM $NaIO_4$ to a 5 mg·ml^{-1} solution of ZR (Melford) in methanol, the solution was incubated for 20 min followed by inactivation with 200 μl of 100 mM ethane 1,2-diol. An aliquot (250 μl) of this solution was stirred with 1 ml of 5 mM biotin-long chain hydrazide in 100 mM sodium acetate, pH 5.5, for 1 h before addition of 50 μl of 10 mg·ml^{-1} sodium cyanoborohydride and incubation at 4 °C overnight. Biotinylated ZR was purified by reverse-phase HPLC.

To avoid the risk that biotinylated compounds in the protein extract might co-purify with the target proteins, naturally biotinylated proteins were removed from extracted protein by dropwise application to a prepared 2 ml monovalent avidin–Sepharose column (Pierce). Extracted protein was cycled through the column 5 times and unbound material was collected and retained for analysis of CK binding. Any bound naturally biotinylated proteins or biotin in the column were removed by washing with 100 mM glycine, pH 2.8. An aliquot (1 ml) of 100 pM biotinylated ZR in Tris buffer (50 mM Tris/HCl, pH 7.2) containing 4 mM glutathionine was then applied to the column in 200 μl aliquots before addition of 1 volume of Tris buffer and incubating overnight at 4 °C. Six volumes of Tris buffer was applied before the unbound stolon tip protein sample was cycled through the column six times. Unbound proteins were removed by sequential washing with Tris buffer containing 4 mM glutathione. The biotinylated ZR–CK binding protein complex was eluted with 8 volumes of Tris buffer containing 2 mM biotin. Protein was 10-fold concentrated by spin dialysis using 10 kDa MWCO centrifugal devices. The N-terminal sequence of the major band of protein was determined after SDS/PAGE and electroblotting on to a PVDF membrane. The band was excised from the membrane and N-terminal Edman sequenced by the Protein and Nucleic Acid Chemistry Facility (Department of Biochemistry, University of Cambridge, Cambridge, U.K.). A 19 amino acid sequence was used in BLASTp and tBLASTn searches for homologues in EST databases of Solanaceae.

StCKP1 (*S. tuberosum* CK riboside phosphorylase 1) nucleic acid sequence extension

Poly(A$^+$) RNA was purified from stolon tips at the IT stage using the Oligotex mRNA Mini kit (Qiagen) and the cDNA sequence extended by RACE-PCR using the Marathon cDNA Amplification kit (Clontech Laboratories). The gene-specific primers used were 5′-TGTCTTTCCACTAATAGCACCATTTGC-3′ and 5′-GAACCATGCAAGCCAAAACC-3′. Amplified 5′ and 3′ RACE-PCR products were cloned into pT7Blue3 (Novagen) and sequenced. Sequences of the fragments were aligned and the region of overlap identified. From this the ORF, 5′-UTR and 3′-UTR of the mRNA were identified for the protein isolated.

Cloning, expression and purification of StCKP1

The predicted CDS (coding DNA sequence) beginning downstream of a predicted signal peptide sequence was cloned into pGADT7 (Clontech) which acted as a donor vector using primers 5′-GAATTCGGAAAGACAAGAAAATTA-3′ and 5′-GGATCCTCAAGCATCTTGATATTTCTT-3′, which also added EcoRI and BamHI restriction sites to the 5′ and 3′ ends of the CDS respectively. The truncated CDS was excised from the donor vector by restriction digest and cloned into pC2X (New England Biolabs) between the EcoRI and BamHI sites to produce a C-terminal fusion protein between maltose-binding protein and the target protein, linked by a Factor Xa protease cleavage site. Constructed plasmids were transformed into *Escherichia coli* strain ER2508 (New England Biolabs) and verified by DNA sequencing before use in protein purification.

Transformants were grown in 500 ml of rich medium [32 g·l^{-1} tryptone, 20 g·l^{-1} yeast extract (>95 % purity, Difco) and 5 g·l^{-1} NaCl] supplemented with 50 mg·ml^{-1} carbenicillin. The cultures were incubated at 37 °C at 3 Hz until D_{600} reached 0.6. Expression of the fusion protein was induced by incubation with 1 mM IPTG at 16 °C for 10 h. Cells were harvested by centrifugation at 8000 ***g*** and resuspended in 10 ml of column buffer (20 mM Tris, pH 7.4, 200 mM NaCl and 1 mM EDTA) before sonication to release soluble proteins. Soluble proteins were collected by

centrifugation at 30000 ***g***, retaining the supernatant. The fusion protein was incubated with amylose slurry and unbound protein was removed by washing the resin with column buffer. The fusion protein was released from the resin by washing with column buffer supplemented with 10 mM maltose. Eluted fusion protein was concentrated 5-fold and transferred into cleavage buffer (100 mM NaCl, 20 mM Tris/HCl and 5 mM $CaCl_2$, pH 7.4) using a 10 kDa MWCO centrifugal device. Recombinant StCKP1 protein was released from the fusion protein by cleavage with 1 % (w/w) Factor Xa. Recombinant StCKP1 was purified by adding the cleavage reaction to amylose slurry and collecting the unbound eluate.

Phylogenetic analysis

The blast homology search algorithms on Spud DB (http://solanaceae.plantbiology.msu.edu/) were used to search the potato genomics resource for transcripts and polypeptides that matched the obtained sequence. The NCBI database (http://www.ncbi.nlm.nih.gov/) of plant sequences and Phytozome (http://www.phytozome.net) were also searched by tBLASTn for homologues of StCKP1 with E values $<1.0\times10^{-75}$. Sequences were aligned using ClustalW Omega and regions not common to all were removed. Evolutionary analyses were carried out in MEGA5 [23]. The evolutionary history was inferred using the neighbour-joining method [24] and 100 bootstrap analyses were carried out [25]. Evolutionary distances were calculated out using the Poisson correction method [26].

Nucleoside phosphorylase assay

The nucleoside phosphorylase assay protocol was developed on the basis of the methods of Chaudhary et al. [27], Kicska et al. [28] and Moshides [29] which could be monitored at set time intervals or continuously to measure deribosylation and ribosylation of CKs respectively. The reaction mixture was a basal mix of 0.5 $g\cdot l^{-1}$ BSA, 30 mM NaF, 1 mM $MgCl_2$ and 50 mM Hepes, pH 5.2, plus supplements dependent on the reaction direction. For the synthetic direction (ribosylation reaction): 4 mM R1-P (ribose 1-phosphate), bis(cyclohexylamine) salt (Sigma–Aldrich) and up to 20 μM CK free base (iP, Z or ZR; Melford) or Ade (Sigma–Aldrich) were included; for the phosphorolytic direction (de-ribosylation reaction): 4 mM K_2HPO_4 (Sigma-Aldrich) and 20 μM CK riboside [iPR and ZR; Melford, DZR (dihydrozeatin riboside), Sigma–Aldrich] or Ado (Sigma–Aldrich). The reaction mixture was pre-warmed to 30 °C before 10 μg of purified recombinant StCKP1 was added as the last component, to a final total volume of 50 μl. Synthetic reactions were monitored by observing the production of ribosylated product from 0.04 μM–20 μM substrate at 285 nm at 5 s intervals in a BioTek Powerwave XS microplate spectrophotometer and allowed to proceed to completion over a 20 min period. To confirm the product of the synthetic reaction, the reactions were terminated by the addition of 5 volumes of 95 % (v/v) ice-cold ethanol and product and unconverted substrate were assayed by RP (reverse-phase)-HPLC. Additional assays containing 20 μM substrate were terminated after a period of 5 min and the remaining substrate and product were confirmed by LC-MS/MS.

De-ribosylation of CK ribosides and Ado over a range of 0.63 μM to 20 μM initial substrate was monitored by stopping the reaction in individual assays by addition of 5 volumes of 95 % (v/v) ice-cold ethanol at 30 s intervals over a total period of 6 min following addition of recombinant protein to a pre-warmed reaction mix. Reaction products were then filtered through a syringe filter, 0.2 μm, and assayed by RP-HPLC. To be comparable with analysis of the ribosylation reaction, additional assays containing 20 μM substrate were terminated after a period of 20 min, and the product and any remaining substrate were assayed by RP-HPLC. As for the synthetic direction, the reactions were also confirmed by LC-MS/MS for a reaction time of 5 min.

RP-HPLC analysis

Separation was on a 150 mm × 4.6 mm column of 5 μm octadecyl silica (Varian Microsorb 100) with a C_{18} guard column, coupled to a Spectraphysics SP8750 pump and SP8700 solvent delivery system and an LC871 UV-VIS detector set at 254 nm to monitor UV absorbance. Isoprenoid CKs were separated on a methanol gradient based on that of Turnbull and Hanke [21]. The column was eluted with a two-solvent gradient: solvent A was 10 % (v/v) aqueous methanol and 80 mM acetic acid, adjusted to pH 3.6 with TEA (triethylamine); solvent B was 80 % (v/v) aqueous methanol and 100 mM acetic acid. The initial condition was 10 % solvent B, rising to 40 % over 20 min, then rising to 60 % between 20 and 30 min and finally held at 60 % between 30 and 35 min. The column was subsequently washed with 100 % methanol for 15 min before equilibrating with 10 % solvent B. Chromatograms were analysed using Chrom Perfect Chromatography Data System (Justice Laboratory Software).

Identification of CKs by MS

CKs were evaporated to dryness, resuspended in 10 μl of acetonitrile and diluted to 200 μl with 10 mM ammonium acetate, pH 3.3. To each sample, a set of deuterium-labelled CK internal standards was added to allow the retention times of likely candidates for MS/MS to be determined. LC-MS analysis of CKs was performed on a Agilent 1100 Binary LC system coupled to an Applied Biosystems Q-Trap hybrid mass spectrometer largely as described by Foo et al. [30]. The LC column was reverse-phase C_{18} (Phenomenex, 3 μm Luna 100 × 2 mm). A TurboIonspray (electrospray) source operating in positive ion mode was used. Data were collected in MRM (multiple reaction monitoring) mode and in full scan MS/MS EPI (enhanced product ion) mode. An EPI channel was included for each substrate and putative product pair. Identification of reaction products was based on co-elution and matching of MS/MS spectra with authentic standards. Estimations of relative quantities of substrate and product were derived from peak areas of MRM signals for each compound pair. Data were processed using Analyst 1.5.1 software (Sciex/Life Technologies).

Construct preparation and generation of transgenic material

For overexpression, the full-length CDS of StCKP1 was amplified using the primers 5′-GAATTCATGGCAATTTCTTCCAAGC-3′ and 5′-GGATCCTCAAGCATCTTGATATTTCTT-3′ and cloned into the binary vector pGreen0029 [31] downstream of a double 35S CaMV (cauliflower mosaic virus) promoter via EcoRI and BamHI restriction sites. The modified region of the binary vector was confirmed by DNA sequencing before introduction into *Agrobacterium tumefaciens* LBA4404 carrying the helper plasmid pSOUP for plant transformation. *S. tuberosum* cv. Desiree was transformed with pGreen0029 (empty vector control) or p35S::StCKP1 according to the methods of Visser [32] and subcultured on MS30 before transfer to soil for tuber production.

PVX:CKP, the agent for gene silencing, was generated by cloning a 437 bp fragment amplified from *StCKP1* cDNA

using primers 5′-AGCAAATGGTGCTATTAGTGGAAAGAC-3′ and 5′-CTTGTGTAATCTCCATTCACTTCAAGC-3′ into the pT7Blue3 (Novagen) subcloning vector. The fragment was excised to the PVX (potato virus X) vector pGR106 [33,34] via AscI and NotI restriction sites with the resultant sequence in antisense orientation. The positive control was construct PVX:PDS containing a 412 bp cDNA fragment of a potato phytoene desaturase gene in antisense orientation enabling silencing to be monitored [35]. White patches on the leaves of positive control PVX:PDS plants confirmed that VIGS (virus-induced gene silencing) was effective under the conditions used. PVX:PDS and pGR106 were gifts from Professor David Baulcombe (Department of Plant Sciences, University of Cambridge). *A. tumefaciens* strain LB4404 carrying the helper plasmid pSoup was transformed with the constructs pGR106 (empty vector control), PVX:PDS or PVX:CKP, and used to infect tuberizing potato plants grown in soil by agroinoculation of leaves [34].

Alteration of *StCKP1* expression was confirmed by RNA blot and RT (reverse transcription)–PCR. RNA was extracted from leaves and tuber periderm of transgenic and infected plants respectively using the Spectrum Plant Total RNA kit (Sigma–Aldrich) and cDNA prepared from 2 μg of RNA by RT. Using the same primers as above, the 437 bp fragment of *StCKP1* was amplified from cDNA prepared from incipiently tuberizing stolon tips, [^{32}P]dATP labelled and used to probe 10 μg of separated total RNA by RNA blot according to the methods of Lewsey et al. [36]. Bound probes were visualized by phosphorimaging and expression was additionally normalized to an 18S rRNA reference probe amplified using primers 5′-CG-CAAATTACCCAATCCTGAC-3′ and 5′-CTATGAAATACGAA-TGCCCCC-3′. Multiplex RT–PCR analysis was carried out on cDNA using primers 5′-ATGCAATTGCCAAAAATCTCG-3′ and 5′-AGCATCTTGATATTTCTTCGA-3′ which amplified a 384 bp fragment of StCKP1, and 5′-AATGTATGGTCCTTGA-CAACG-3′ and 5′-CACCTGTCTACCAATGCAAG-3′ which amplified a 609 bp fragment of β-tubulin. Quantified gel band intensities for *StCKP1* were standardized against β-tubulin for each reaction in exponential phase. This process was repeated for each of three separate cDNA samples produced from extracted RNA.

Phenotypic analysis of tubers and tuber induction

Microtubers were induced from single nodes in the absence of exogenous CK according to a method adapted from Gopal et al. [37]. Single nodal segments (5–10 mm) with subtending leaf were taken from 6–8-week-old aseptically grown plantlets and placed in PMM [1 × Murashige and Skoog basal salts, 6 % (w/v) sucrose, pH 5.8 and 0.8 % phytoagar] in the dark at 21 °C. Emergent stolons were monitored daily for signs of tuberization and judged to have tuberized when the tip had swollen to three times the diameter of the stolon.

Immediately after harvest from soil, tubers were weighed and photographed for measurement of length and width using ImageJ (NIH). Tuber length was determined as the longest measurable span across the tuber axis. Tuber width was measured at right angles to the length measurement and taken halfway along the tuber length to calculate the length to width ratio for each line.

Tubers were categorized by mass into 3 classes: 5–$\leqslant$20 g, 20–$\leqslant$40 g and >40 g. Tubers weighing <5 g were discarded. Sets of tubers containing five tubers of each size class were given one of two alternative treatments. One set of tubers was placed immediately at 16 °C in darkness whereas a second set was stored in darkness at 4 °C for 21 days, a 'chill' treatment, prior to transferring to dark storage at 16 °C. Tubers were monitored twice weekly for dormancy break, defined by sprouts from apical or lateral buds reaching 3 mm in length.

Table 1 The effects of 2000-fold excesses of unlabelled compounds on ZR-[^{3}H]diol binding by partially purified potato stolon tip protein (50–75 % ammonium sulfate 'cut'), mean values of results from duplicate experiments

Compound	Displacement (%)
ZR-diol	~100
ZR	~100
Z	~100
DZR	93
Ade	41.5
Ado	37

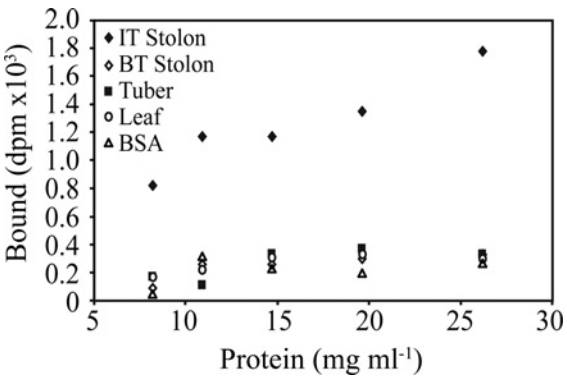

Figure 2 ZR-[^{3}H]diol binding by partially purified (50–75 % ammonium sulfate 'cut') protein samples from potato cv. Majestic tissues

Each point is the mean of results from duplicate experiments. IT Stolon, incipiently tuberizing stage stolon tips (9 months post-harvest, no sign of apical swelling); BT Stolon, stolon tips before tuberizing (6 months post-harvest); Tuber, storage pith from mature tubers; Leaf, young leaves from plants in the field. A BSA control shows the background binding.

RESULTS AND DISCUSSION

Potato stolon tips have CK-binding activity

Protein from incipiently tuberizing stolon tips (IT) bound approximately 8-fold more ZR-[^{3}H]diol per mg of protein than protein from the morphologically identical stolons 3 months prior to this stage (BT; Figure 2). In the presence of a 2000-fold molar excess of unlabelled ZR-diol, binding of the radiolabelled ZR-[^{3}H]diol ligand was reduced to a level comparable with non-specific binding. The competitive effects of other compounds were measured relative to this standard (Table 1). Unlabelled native CKs ZR and Z were highly effective at preventing ZR-[^{3}H]diol binding, and the CK DZR was almost as effective. In contrast, the non-CK structural homologues Ade and Ado inhibited the binding of ZR-[^{3}H]diol much less than excess CKs, indicating preferential binding of CKs over non-CKs. The affinity of the CK binding for ZR-[^{3}H]diol was estimated by Scatchard analysis (see Supplementary Figure S1 at http://www.biochemj.org/bj/458/bj4580225add.htm). The binding site concentration in the extract was calculated to be 30 nM with a dissociation constant (K_d) of 1.7×10^{-7} M for ZR-[^{3}H]diol and an estimated binding site concentration of approximately 70 pmol·g^{-1} FM of stolon tips.

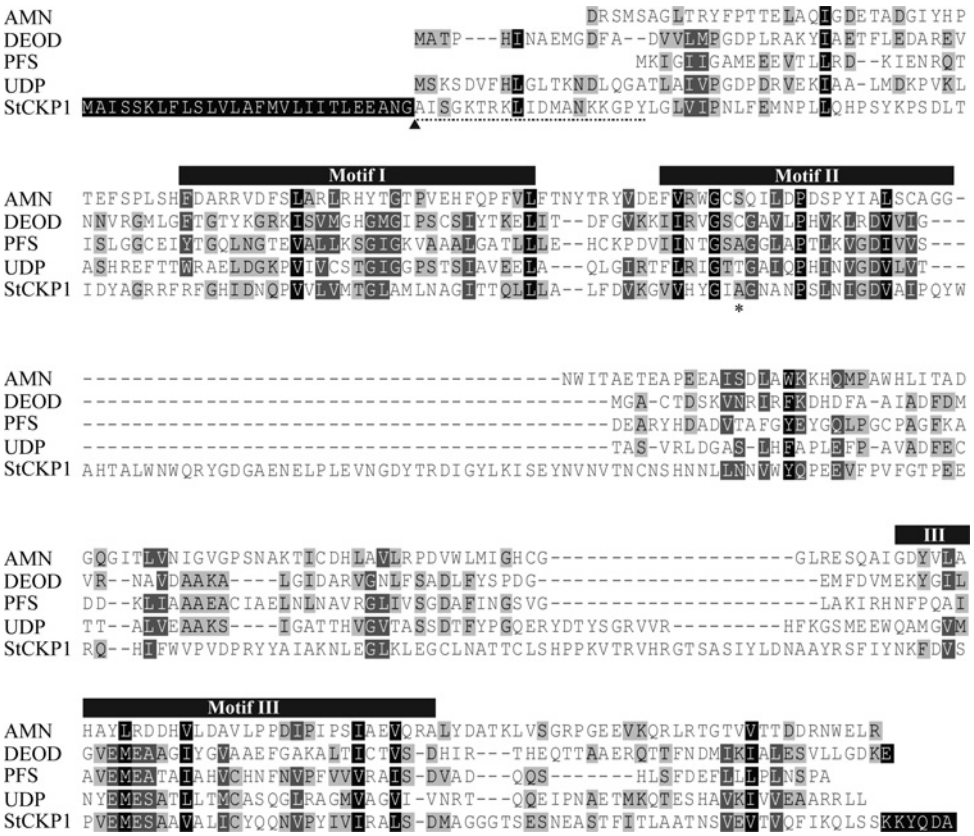

Figure 3 Predicted amino acid sequence of StCKP1 aligned with four different family 1 nucleosidases from *E. coli*: AMP hydrolase (AMN), purine phosphorylase (DEOD), methylthioadenosine/*S*-adenosylhomocysteine nucleosidase (PFS) and uridine phosphorylase (UDP) [22]

The 19 amino acid sequence determined by N-terminal sequencing is underlined. Positions of the conserved motifs I, II and III are annotated with boxes above. The position of the alanine residue in motif II is highlighted with an asterisk. Predicted signal peptide cleavage site = ▲.

The major CK-binding protein is a member of a nucleosidase and nucleotidase superfamily

The CK-binding protein fraction isolated from IT stage stolon tips was analysed by SDS/PAGE (Supplementary Figure S2 at http://www.biochemj.org/bj/458/bj4580225add.htm). The most prominent band of protein had an estimated relative molecular mass of 40 kDa. An unambiguous 19 amino acid N-terminal sequence was obtained from the band.

Significant homology was found between the amino acid sequence and translated EST sequences from the potato, tomato and tobacco databases, including roots, flower buds, germinating seedlings, shoot meristems, stolons, sprouting eyes of potato tubers and microtubers. Primers designed for the consensus regions of the ESTs were used to amplify a partial gene fragment from cDNA prepared from IT stage stolon tips, which was then extended by RACE-PCR, cloned and sequenced. A potential long ORF from the nucleotide in position 54 to a termination codon at position 1116 encoded a predicted polypeptide of 354 residues, with calculated molecular mass of 39.3 kDa. The closest match for the predicted polypeptide sequence is the representative transcript/peptide sequence for the locus Sotub08g016060.1.1 (Spud DB). The translation product has a predicted signal peptide of 27 residues likely to be removed during processing [38], leaving a mature polypeptide of 327 residues, calculated molecular mass 36.4 kDa. The N-terminus of the predicted product of processing was confirmed to match the 19 amino acid sequence determined previously. As the amino acid sequence includes a cleavable signal peptide (Figure 3), but not an unambiguous transmembrane-spanning domain, we infer that the protein is apoplastic, either in the cell wall or the lumen of the ER. These properties are consistent with the soluble nature of the binding activity.

The full-length amino acid sequence includes three distinct conserved motifs (I, II and III) associated with enzyme activity of a class of bacterial nucleosidases (Figure 3), described by Mushegian and Koonin [39], who predicted that the probability of obtaining each of the conserved motifs by chance alone was less than 10^{-5}. The predicted amino acid sequence of the potato protein differs from the consensus sequence for both motifs I and II at two positions (Figure 3), but matches the consensus sequence for motif III. The functions of motifs I and III are unknown, but conserved motif II shows low similarity to the ribose-binding motif of eukaryotic nucleoside phosphorylases. In particular, the potato protein motif II includes a conserved alanine residue between two β-sheets (asterisk in Figure 3), a central feature of the active centre of a human purine nucleoside phosphorylase in which it forms a hydrogen bond with the ribosyl 3′-hydroxyl [40].

The expressed protein has purine riboside phosphorylase activity on CK substrates

A hybrid gene was constructed containing *malE* fused to the CDS of *StCKP1*, truncated by omission of the predicted signal peptide sequence, and the protein expressed in *E. coli* cells. The expressed protein was extracted and cleaved from MalE using Factor Xa, and purified to yield the target protein. An end-point assay was used to assay for nucleosidase activity

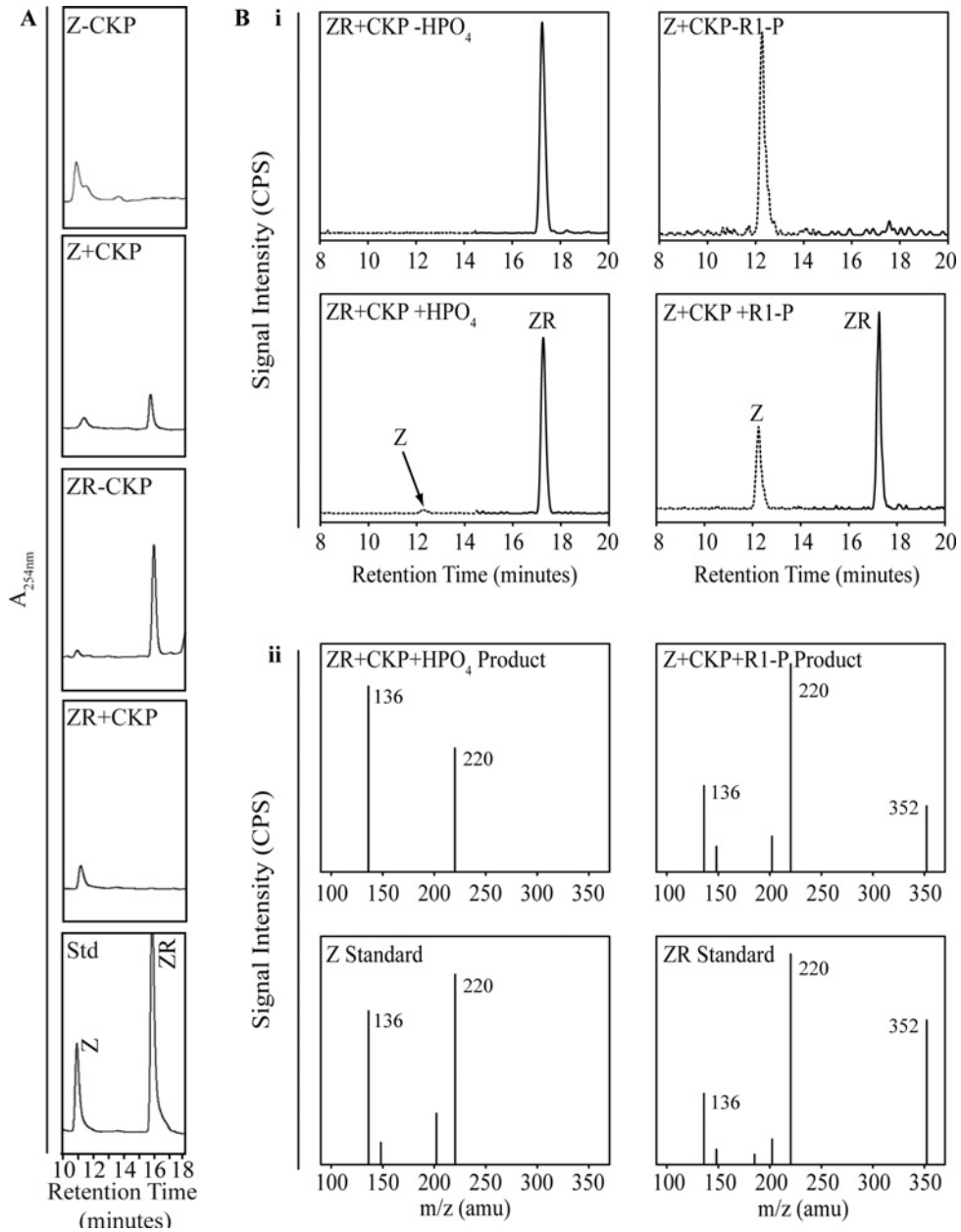

Figure 4 Phosphorylase activity of recombinant StCKP1, in the synthetic and phosphorolytic directions, on Z and ZR as substrates

(**A**) RP-HPLC analysis of products: Z + CKP, Z plus R1-P and protein; Z-CKP, no-protein control; ZR + CKP, ZR plus P_i and protein; ZR-CKP, no-protein control; Std, standard. Reactions were stopped after 20 min incubation with 20 μM substrate. (**B**) i, LC-MS/MS EPI full-scan total ion chromatograms of products from reactions terminated after 5 min. Broken lines represent data collected in the *z* channel (MS/MS of *m*/*z* 220), and solid lines in the ZR channel (MS/MS of *m*/*z* 352). Left-hand panels show requirement for P_i in conversion of ZR into Z and right-hand panels show requirement for R1-P in conversion of Z into ZR. ii, MS/MS spectra confirming identities of reaction product peaks from panel i and corresponding authentic standards. Left-hand panel shows Z spectra (retention time 12.29 min) and right-hand panel shows ZR spectra (17.27 min). Z + CKP + R1-P, Z plus R1-P and protein; Z + CKP-R1P, no-R1-P control; ZR + CKP + HPO_4, ZR plus P_i and protein; ZR + CK-HPO_4, no-P_i control. amu, atomic mass unit.

predicted by the structural homology with known nucleosidases. Appropriate substrates were selected for the direction of reaction being measured. When assaying for phosphorolytic activity, the assay mix was supplemented with 4 mM K_2HPO_4 as a phosphate donor and 20 μM CK riboside substrate, iPR, ZR or DZR. When assaying for ribosyltransferase activity, the assay mix was supplemented with 4 mM R1-P as a ribosyl donor and 20 μM CK base, iP, Z or DZ (dihydrozeatin). Reactions were halted after 20 min at 30 °C, and products assayed by RP-HPLC together with CK standards and reaction controls. In the presence of excess inorganic phosphate, the expressed protein catalysed the transfer of a ribosyl moiety from the riboside to produce the corresponding CK base (Figure 4A). In the absence of added P_i, no cleavage was detected (results not shown). With excess R1-P and a CK base, the expressed protein catalysed formation of the corresponding riboside (Figure 4A). In the absence of added R1-P, no reaction was detected (results not shown). Reaction controls using 10 μg of maltose-binding protein purified from induced *E. coli* cells expressing the pMalc2x vector showed no detectable activity with any combination of substrates (results not shown).

LC-MS/MS unambiguously confirmed the identities of the reaction products. Substrates and products with parent ions at *m*/*z*

of 352 and 220 were monitored for reciprocal reactions involving ZR and Z (Figure 4B). Similarly, parent ions at *m*/*z* 336 and 204 were used to monitor iPR and iP (Supplementary Figure S3 at http://www.biochemj.org/bj/458/bj4580225add.htm), and parent ions at *m*/*z* 354 and 222 for DZR and DZ (Supplementary Figure S4 at http://www.biochemj.org/bj/458/bj4580225add.htm). Reaction products with a given parent ion *m*/*z* and a retention time that correlated with corresponding internal standards were fragmented, and the resultant MS/MS spectrum compared with that of CK base and riboside standards. Detection of phosphorolysis and ribosyltransferase activity by LC-MS/MS was in complete agreement with the results of the RP-HPLC analysis. Two CK types were found in each reaction mix: product and substrate. In the case of phosphorolysis, MS/MS spectra for the major product corresponded to the CK base derived from its riboside substrate. This confirmed the riboside-into-base conversion. For ribosylation, the spectra for the major product were identified as the CK ribosides corresponding to each CK base substrate, likewise confirming the conversion of base into riboside. Quantification of substrate/product pairs identified by LC-MS/MS according to the ratio method outlined by Prinsen et al. [41] indicated that, given the same concentration of CK substrate with excess co-substrate, the expressed protein acted preferentially as a ribosyltransferase (Figure 5).

On the evidence of these results, we propose the gene name *StCKP1* (*S. tuberosum* CK riboside phosphorylase 1) for the sequence encoding the enzyme identified, from which we derive the abbreviation 'CKP' for CK riboside phosphorylase.

StCKP1 shows a preference for CK over Ade substrates

Ribosylation and phosphorolysis were monitored over time to determine kinetic constants for expressed StCKP1. Purine nucleoside phosphorylase activity has previously been followed by spectrophotometric analysis of substrate disappearance [27,28]. Absorbance at 1 nm intervals between 200 and 500 nm of 20 μM solutions of each CK species was measured, and 285 nm was determined as the wavelength at which there was the largest difference between absorbance of base and riboside (Supplementary Figure S5 at http://www.biochemj.org/bj/458/bj4580225add.htm). The method proved to be useful for assaying riboside as product generated, but not for riboside as substrate consumed during phosphorolytic reactions. Thus the ribosylation reaction was monitored spectrophotometrically over a 20 min time course. Phosphorolysis was monitored by an end point assay, terminating the reaction after a given time by addition of an equal volume of ethanol to precipitate the protein, filtering and analysing the reaction mixture by RP-HPLC. The Michaelis–Menten constants for ribosylation were determined using the nucleosidase assay described above for the CK bases iP, Z and DZ over the concentration range 0.08–20 μM. Ade was also offered as a substrate since purine nucleoside phosphorylases are thought to be primarily enzymes of the Ade salvage pathway [42]. For each substrate concentration, the change in absorbance units per second for the first 200 s of the reaction was measured and corrected by the gradient of the standard curve for each CK to give picomol of riboside formed per second. The initial rate (V_0) was expressed as a specific enzyme activity per picomol of protein. A hyperbolic curve was fitted to calculated values for V_0 according to the Michaelis–Menten equation [43], which allowed determination of a K_m value of 0.35 μM for Z (Figure 6A), 0.053 μM for iP and 0.56 μM for DZ (Table 2). A K_m value for Ade of 3.3 μM was determined, indicating that the expressed protein can use Ade, but has a higher affinity for CK base substrates, in line with the characteristics of binding activity in crude protein from IT stage stolon tips (Table 1).

Phosphorolysis of CK ribosides and Ado was monitored over a range of 0.63 μM to 20 μM with the lower bounds of detection being limited by the sensitivity of the detector. Reaction products were separated by RP-HPLC and quantified relative to a standard curve. V_0 was determined from the initial gradient of free base produced and expressed as a specific enzyme activity per picomol of protein. K_m values determined were 7.2 μM for ZR (Figure 6B),13.3 μM for iPR, 7.7 μM for DZR and 128 μM for Ado (Table 2).

Taken together, the data indicate that the purine riboside phosphorylase activity of the expressed sequence has a higher affinity for CKs than for the unsubstituted aminopurines Ade and Ado, justifying its designation as an authentic CK riboside phosphorylase.

The characteristics of the activity of the expressed protein were broadly similar to those of the CK-binding activity of stolon tip protein from the IT stage of development. First, CKs were preferred over Ade and Ado. Secondly, although generally less active as a hormone [44], the CK metabolite DZR interacted effectively with the binding activity and was also a good substrate for the enzyme. Thirdly, not just aminopurines but also their ribosides were both ligands for binding and substrates for the enzyme. Finally, the K_d value for ZR-diol, a modified version of ZR that retains an unmodified Z moiety, in the binding assay was of the same order as the apparent K_m value for Z in the enzyme assay. On the basis of this evidence, we propose that the binding activity of stolon tips is due to StCKP1. In view of its high affinity and selectivity for CKs, and its similarity to the binding activity from plant tissue, it is unlikely that activity of recombinant StCKP1 was aberrant as a consequence of expression in a prokaryote.

This is only the second time that CK riboside phosphorylase activity has been reported for a plant, and the characteristics of StCKP1 differ from those of the wheat germ nucleoside phosphorylase activity identified by Chen and Petschow [14]. First, StCKP1 had a lower apparent K_m value for both Ade and iP than the activity from wheat germ; and secondly, StCKP1 prefers CK substrates to Ado/Ade in contrast with the wheat germ activity. The apparent K_m values suggest that the wheat germ enzyme interconverts Ade and Ado as intermediary metabolites whereas StCKP1 contributes to the interconversion of free base and riboside forms of CKs as hormones.

All attempts to find Ado phosphorylase and CK riboside phosphorylase activities in plants suggest that they are normally present at undetectably low levels [45,46]. Negative results are much less likely to be reported, therefore it is noteworthy that, from a careful study of the close potato relative tomato, Ado phosphorylase was the only known purine interconverting enzyme activity that Burch and Stuchbury [45] could not detect. We detected CK-binding activity in only one type of tissue of potato, stolon tips, at one stage in development, just prior to tuberization (Figure 2, IT). It may be that the enzyme is only active in small groups of cells or at restricted stages in development, or a combination of both, perhaps reflecting the importance of restricting the interconversion of base and riboside to control points in development. A specialised role could, however, be common to a wide range of plants. A preliminary survey indicates that the genomes of all higher plants that we have searched contain genes for homologues sharing unique features with *StCKP1* (Supplementary Figure S6 at http://www.biochemj.org/bj/458/bj4580225add.htm), but whether the homologous proteins have similar enzyme activity remains to be demonstrated.

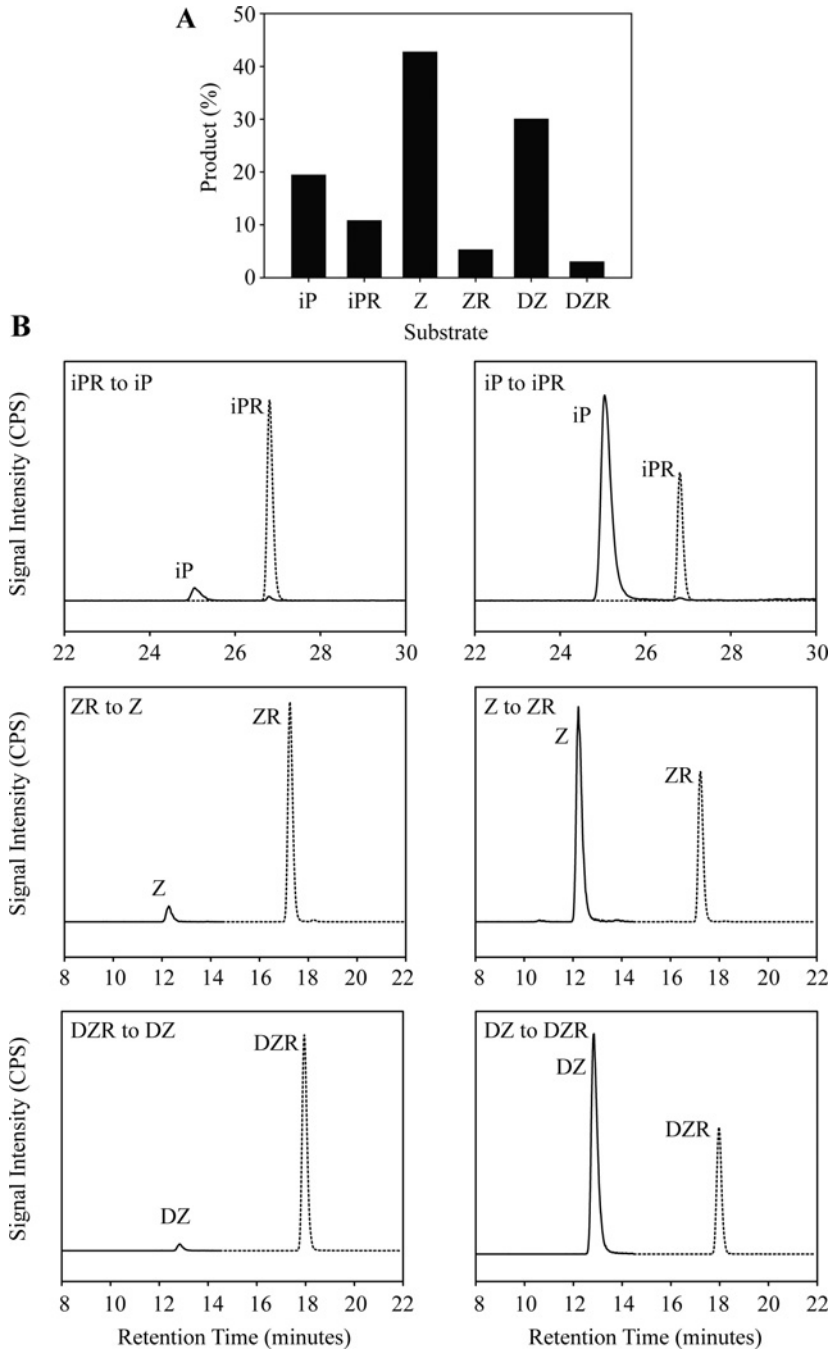

Figure 5 Estimated relative conversion of StCKP1 substrates into products after a 5 min reaction time

(**A**) Product abundance expressed as the percentage of total peak areas from sum of substrate and product analysed by LC-MS-MRM. (**B**) Extracted MRM chromatograms from LC-MS-MRM analysis of each reaction, showing detection of product and substrate peaks, all at expected retention times on the basis of analysis of authentic standards. MRM transitions monitored were (*m*/*z*): iP, 204/136 (continuous line); iPR, 336/204 (broken line); Z, 220/136 (continuous line); ZR, 352/220 (broken line); DZ, 222/136 (continuous line); and DZR, 354/222 (broken line).

StCKP1 is a positive regulator of chill-responsive tuber endodormancy

To investigate the biological role of StCKP1, the expression of the gene in potato plants was altered and the effects on the phenotype of the plants examined. A modified PVX VIGS system was used to down-regulate *StCKP1* expression, and constitutive expression from the 35S CaMV promoter to up-regulate expression. Tuber buds were monitored for altered dormancy characteristics since CKs play a role in both entry to and departure from the endodormant state [16–19].

Down-regulating *StCKP1* expression by VIGS shortened tuber dormancy; up-regulation by 35S-driven expression prolonged tuber dormancy. In both cases, the alteration in the length of dormancy was attributable to an alteration in the chill-responsive component (Figure 7A), calculated as the difference between the average duration of endodormancy for tubers stored at 16 °C and the average duration of endodormancy for tubers kept for 21 days

Table 2 Values for the calculated enzyme constants of heterologously expressed StCKP1 for free base substrates undergoing ribosylation, and for riboside substrates undergoing phosphorolytic cleavage

Substrate	K_m (μM)	k_{cat} (s^{-1})
Ribosylation		
iP (+R1-P)	0.053	0.408
Z (+R1-P)	0.354	0.373
DZ (+R1-P)	0.562	0.386
Ade (+R1-P)	3.33	0.213
Phosphorolytic cleavage		
iPR (+P_i)	13.31	0.408
ZR (+P_i)	7.22	0.018
DZR (+P_i)	7.71	0.078
Ado (+P_i)	128	0.460

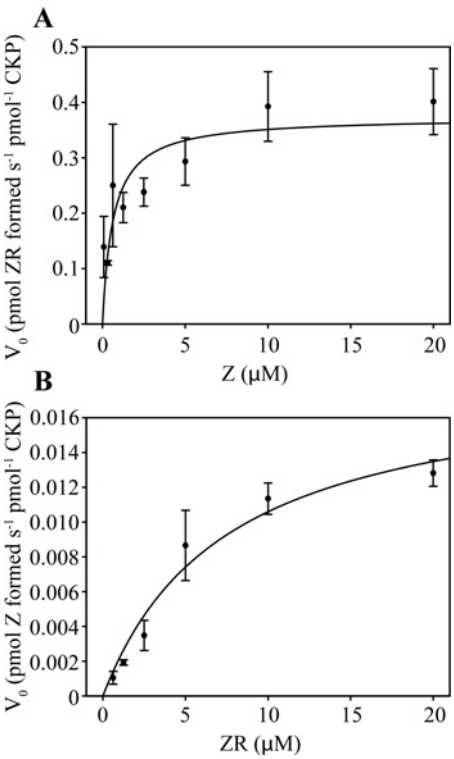

Figure 6 Kinetic plots of StCKP1 activity with Z substrates

(**A**) Synthesis of ZR from Z and R1-P. (**B**) Phosphorolytic cleavage of ZR to form Z. CKP, recombinant StCKP1 protein.

at 4 °C prior to storage at 16 °C. Across the lines generated, the lower the abundance of *StCKP1* transcripts in the tuber periderm, the shorter the time before buds sprouted; likewise, the greater the abundance of *StCKP1* transcripts, the longer the time before tuber buds sprouted. In some cases, up-regulation of StCKP1 prolonged the chill-responsive component by an average of 40 days whereas reduction of StCKP1 to 25 % of control lines almost eliminated this component. The Pearson product-moment correlation coefficient was calculated to assess the relationship between *StCKP1* expression and the contribution of the chill-responsive component to dormancy. In both approaches, a positive correlation was observed between the two variables (*StCKP1* down-regulation: $r^2 = 0.83$, $P = 0.006$; *StCKP1* up-regulation: $r^2 = 0.89$, $P = 0.04$). The loss of the chill-reversible component on down-regulating *StCKP1* suggests that StCKP1 activity is necessary for tuber buds to maintain the endodormant state for the characteristic time. The lengthening of dormancy by overexpression demonstrates that extra StCKP1 activity alone is sufficient for tuber buds to maintain the endodormant state for longer than that of non-transgenic Desiree. Our results therefore indicate that StCKP1 is a dormancy-promoting factor.

Comparison of dormancy duration for chill-treated and unchilled tubers from the same plant showed that in both cases the residual dormancy of chill-treated tubers was not detectably affected by alteration of *StCKP1* abundance, remaining the same as controls (Supplementary Figure S7 at http://www.biochemj.org/bj/458/bj4580225add.htm). This finding suggests that the mechanism determining the duration of endodormancy in chill-treated tubers does not involve StCKP1. Instead, StCKP1 appears to have a rather specific role as a regulatory component of the dormancy-shortening response to chill treatment whose expression is directly related to the duration of a chill-alleviable contribution to the total duration of tuber endodormancy.

The characteristics of the physiological activity of StCKP1 match the insensitivity of tuber bud dormancy to exogenous CK previously reported for cv. Majestic. For unchilled tubers, CK insensitivity was maintained up until a few days before spontaneous sprouting revealed the end of endodormancy. Chill treatment shortened the time before endodormancy ended in response to an accelerated increase in bud CK up to active levels [18,21].

CKs are prime endogenous negative regulators of potato tuber dormancy [18,19], which allows us to conclude that in this case StCKP1 is acting to oppose its substrate/ligand CK, i.e. StCKP1 prolongs dormancy by lowering CK activity. That makes it less likely that the enzyme is working in the phosphorolytic direction here, which would release the more active free base. This is in line with the K_m values determined by *in vitro* assay which indicate that the affinity of the protein for the free bases is higher than that for the ribosides (Table 2) and, supplied with equivalent concentrations of substrates, the reaction preferentially generated ribosides from the free bases (Figure 5). Two possibilities remain: first, StCKP1 down-regulates the activity of the free base form of CK by enzymic conversion into the less active riboside; and secondly, StCKP1 inactivates either form of CK by binding the hormone, making it inaccessible to its receptor. We note that enzymes catalysing two-substrate reactions cannot proceed beyond binding the first substrate if the second substrate (in this case R1-P) is not available [47]. At 70 pmol·g^{-1} FM, the StCKP1 content of stolon tips as they enter dormancy is greater than the tissue content of CKs: 40 pmol·g^{-1} FM [21]. We suggest that sequestration of CK by high-affinity binding is a feasible mechanism for local and specific inactivation of CK by StCKP1 in potato.

Our earlier analyses of the zeatin CKs in tuber tissues of cv. Majestic at successive stages of the tuber cycle are consistent with both of the suggested mechanisms operating at different stages. Throughout the growth stage, tubers are endodormant even though the content of zeatin CKs was high, up to 170 pmol·g^{-1} FM. Almost all of this was as the riboside, suggesting that in growing tubers StCKP1 may promote endodormancy by converting CKs into ribosides. Dormancy continues after tuber maturation, associated with low levels of CK and lack of response to exogenous CKs. In this state, conversion of injected zeatin riboside or zeatin free base into other CK forms was suppressed. Later, when dormancy is lost and CK responsiveness regained, added CK now became redistributed between ribotide, free base and riboside (compare Figures 6 and 7 in [21]). Sequestration of both free base and riboside forms of CK by binding to StCKP1 could explain the block on interconversion in post-harvest tubers

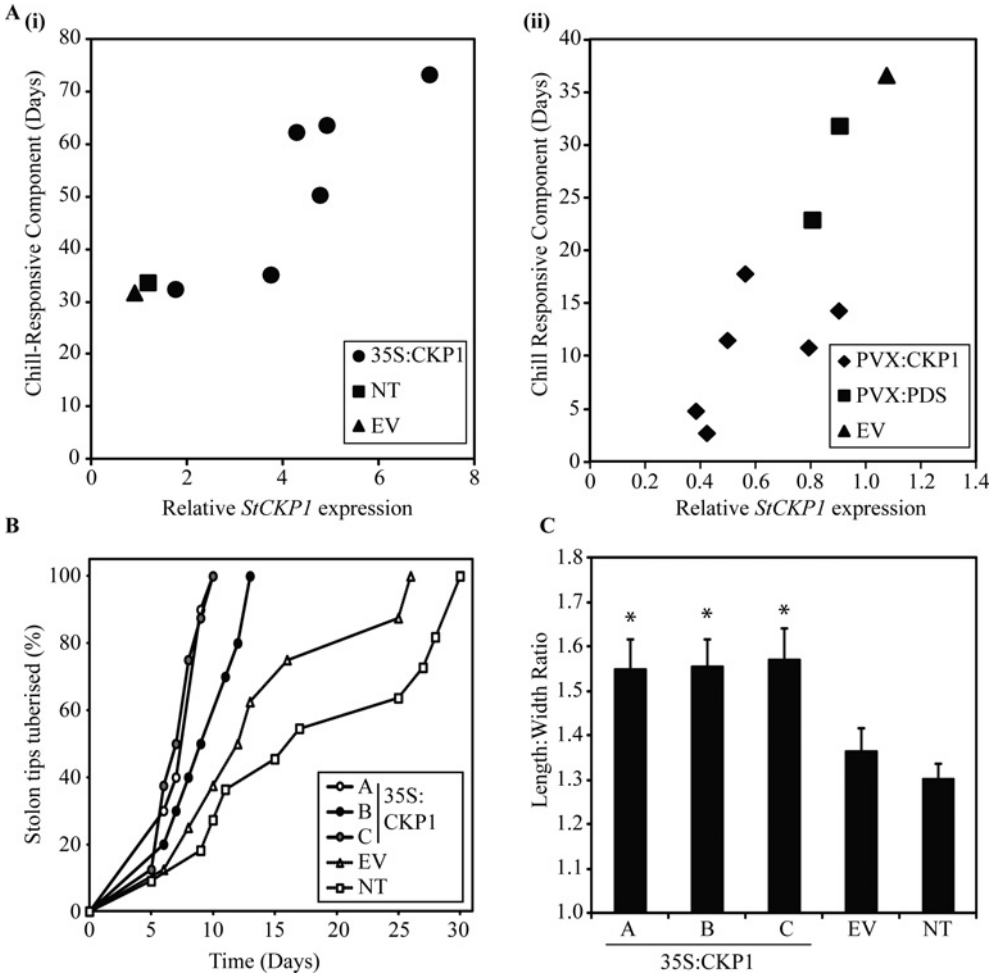

Figure 7 Effects of altered expression of *StCKP1* on tuber phenotype

(**A**) Contribution of chill-responsive component of dormancy when *StCKP1* was: (i) up-regulated by overexpression from the 35S promoter; and (ii) down-regulated by VIGS. The results are mean duration of endodormancy for 15 tubers, 5–40 g of FM, harvested from a single plant. Each individual plant represents a separate transformation or infection event. *StCKP1* expression was normalized to non-transformed controls for overexpressing lines (NT = 1.0) and normalized to empty vector controls for VIGS lines (EV = 1.0). (**B**) Microtuberization of stolons induced from single nodal explants. The results shown are the mean of three experiments. (**C**) Length/width ratios of all tubers harvested from a single plant of each line. The results are means ± S.D., $n \geqslant 45$. Three representative transgenic lines are shown in (**B**) and (**C**). EV, empty vector transgenic/ infected control; NT, non-transformed.

as they remain endodormant, and account for both their CK insensitivity and their endodormant state.

Regulating the duration of dormancy appears to be the main contribution of StCKP1 to survival

Close observation of PVX:StCKP1-infected plants and 35S:StCKP1-overexpressing lines, in aseptic shoot culture and in pots of soil, throughout the growing period through to senescence showed no detectable differences from the uninfected non-transgenic parental plants. Particular attention was paid to aspects of development known to be affected by CKs: chlorophyll content, root growth, shoot branching and leaf senescence [1]. Apart from effects on dormancy, we could detect only two other differences in phenotype between 35S:StCKP1-overexpressing lines and control lines. Both relate to the tuber.

First, *StCKP1* overexpression promoted tuber induction *in vitro*. The axillary bud of single node explants in aseptic culture in the light with 3 % sucrose as carbohydrate source grows out as a leafy shoot branch. In the dark with 6 % sucrose as carbohydrate source [37], the axillary bud grows out as a stolon, the tip of which forms a small tuber. For explants of non-transgenic Desiree, tubers were initiated at some point between 5 and 30 days after explanting. By contrast, in the same conditions all lines over-expressing *StCKP1* initiated tubers between 5 and 12 days after explanting (Figure 7B). StCKP1-overexpressing lines initiated tubers at an average rate of 0.72 tubers/day as compared with non-transformed and empty vector control lines which initiated tubers at a rate of 0.31 and 0.32 tubers/day respectively. Analysis of covariance shows a significant difference ($P < 0.0001$) in the rate of tuberization for all overexpressing lines relative to both controls. This result appears to reflect another aspect of the same dormancy-prolonging activity of StCKP1: extending the duration of dormancy by advancing the start in addition to delaying the end.

Secondly, all of the *StCKP1*-overexpressing lines produced slightly elongated tubers relative to controls. The effect is small, but significant, when analysed by a Student's *t* test (Figure 7C and Supplementary Figure S8 at http://www.biochemj.org/bj/458/bj4580225add.htm). The biological consequences of *StCKP1* expression appear to be confined to the tuber phase even when the gene is expressed constitutively.

Homologues of *StCKP1* are present in many other plant taxa (Supplementary Figure S6). Although potato and its close relative tomato have only a single syntenic copy, some dicots appear to have two paralogues, and poplar possesses the alternative paralogue to StCKP1 only. Cereals have a distinctive pair of paralogues. Some of these genes may contribute to the duration of endodormancy in buds, and possibly seeds, in species other than potato.

AUTHOR CONTRIBUTION

Jennifer Bromley developed enzyme assays, identified reaction products, determined kinetic constants, generated and characterized overexpressing potato lines, prepared the Figures, and co-wrote and co-edited the paper before submission. Barbara Warnes identified full-length StCKP1, expressed StCKP1 in *E. coli*, detected enzyme activity, and generated the VIGS potato lines. Christine Newell characterized the VIGS potato lines. Jamie Thomson characterized stolon tip cytokinin-binding activity. Celia James isolated the stolon tip cytokinin-binding protein. Colin Turnbull discovered the stolon tip cytokinin-binding protein activity, generated and interpreted MS data, and co-edited the paper. David Hanke obtained funding, conceived and planned the investigation, interpreted the data, and co-wrote and co-edited the paper before submission.

ACKNOWLEDGEMENTS

We thank Sue Green for superb technical asistance throughout, Olga Sedelnikova for assistance with enzyme assay development, Chris White for assistance with phylogenetic interpretation and Mark Bennett at Imperial College for help with LC-MS/MS. We also thank the skilled work of Alex Goodall and Pete Michna, and their staff at the University of Cambridge Botanic Garden who for the past 35 years have grown the potato tubers that were used in this investigation.

FUNDING

This work was funded by the Department of Agriculture and Fisheries for Scotland [grant number 5378/79/33] the UK Biotechnology and Biological Sciences Research Council (BBSRC) [grant number 8/C 01401], the UK Department for Environment, Food and Rural Affairs Sustainable Arable LINK scheme [grant number LK09105], the UK Research Councils' 'Follow-on' Fund, [grant number BB/FOF/207], the UK Potato Council-sponsored BBSRC CASE Studentship [grant number R271] and the Isaac Newton Trust [grant number MINUTE 6.08(P)].

REFERENCES

1 Sakakibara, H. (2006) Cytokinins: activity, biosynthesis and translocation. Annu. Rev. Plant Biol. **57**, 431–449
2 Kudo, T., Kiba, T. and Sakakibara, H. (2010) Metabolism and long distance translocation of cytokinins. J. Integr. Plant Biol. **52**, 53–60
3 Stolz, A., Riefler, M., Lomin, S. N., Achazi, K., Romanov, G. A. and Schmulling, T. (2011) The specificity of cytokinin in *Arabidopsis thaliana* is mediated by differing ligand affinities and expression profiles of the receptors. Plant J. **67**, 157–168
4 Sun, J., Hirose, N., Wang, X., Wen, P., Xue, L., Sakakibara, H. and Zuo, J. (2005) *Arabidopsis* SOI33/AtENT8 gene encodes a putative equilibrative nucleoside transporter that is involved in cytokinin transport in plants. J. Integr. Plant Biol. **47**, 588–603
5 Kuroha, T., Tokunaga, H., Kojima, M., Ueda, N., Ishida, T., Nagawa, S., Fukuda, H., Sugimoto, K. and Sakakibara, H. (2009) Functional analyses of LONELY GUY cytokinin-activating enzymes reveal the importance of the direct activation pathway in *Arabidopsis*. Plant Cell **21**, 3152–3169
6 Kwade, Z., Świątek, A., Azmi, A., Goosens, A., Inzé, D., Van Onckelen, H. and Roef, L. (2005) Identification of four adenosine kinase isoforms in tobacco BY-2 cells and their putative role in the cell cycle-regulated cytokinin metabolism. J. Biol. Chem. **280**, 17512–17519
7 Zhang, X., Chen, Y., Lin, X., Hong, X., Zhu, Y., Li, W., He, W., An, F. and Guo, H. (2013) Adenine phosphoribosyl transferase 1 is a key enzyme catalyzing cytokinin conversion from nucleobases to nucleotides in *Arabidopsis*. Mol. Plant **6**, 1661–1672
8 Chen, C. M. and Kristopeit, S. M. (1981) Metabolism of cytokinin: dephosphorylation of cytokinin ribonucleotide by 5′-nucleotidases from wheat germ cytosol. Plant Physiol. **67**, 494–498
9 Schoor, S., Farrow, S., Blaschke, H., Lee, S., Perry, G., von Schwartzenberg, K., Emery, N. and Moffatt, B. (2011) Adenosine kinase contributes to cytokinin interconversion in *Arabidopsis*. Plant Physiol. **157**, 659–672
10 Burch, L. R. and Stuchbury, T. (1986) Purification and properties of adenosine nucleosidases from tomato (*Lycopersicon esculentum*) roots and leaves. J. Plant Physiol. **125**, 267–273
11 Riewe, D., Grosman, L., Fernie, A. R., Zauber, H., Wucke, C. and Geigenberger, P. (2008) A cell wall-bound adenosine nucleosidase is involved in the salvage of extracellular ATP in *Solanum tubersosum*. Plant Cell Physiol. **49**, 1572–1579
12 Jung, B., Florchinger, M., Kunz, H. H., Traub, M., Wartenberg, R., Jeblick, W., Neuhaus, H. E. and Mohlmann, T. (2009) Uridine-ribohydrolase is a key regulator in the uridine degradation pathway of *Arabidopsis*. Plant Cell **21**, 876–891
13 Chen, C. M. and Kristopeit, S. M. (1981) Metabolism of cytokinin: deribosylation of cytokinin ribonucleoside by adenosine nucleosidase from wheat germ cells. Plant Physiol. **68**, 1020–1023
14 Chen, C. M. and Petschow, B. (1978) Metabolism of cytokinin: ribosylation of cytokinin bases by adenosine phosphorylase from wheat germ. Plant Physiol. **62**, 871–874
15 Holub, J., Hanuš, J., Hanke, D. E. and Strnad, M. (1998) Biological activity of cytokinins derived from *ortho*- and *meta*-hydroxybenzyladenine. Plant Growth Regul. **26**, 109–115
16 Palmer, C. E. and Smith, O. E. (1969) Cytokinins and tuber initiation in the potato *Solanum tuberosum* L. Nature **12**, 279–280
17 Tao, G.-Q., Letham, D. S., Yong, J. W. H., Zhang, K., John, P. C. L., Yong, J. W. H., Schwartz, O., Wong, S. C. and Farquhar, G. D. (2010) Promotion of shoot develpment and tuberisation in potato by expression of a chimaeric cytokinin synthesis gene at normal and elevated CO_2 levels. Funct. Plant Biol. **37**, 43–54
18 Turnbull, C. G. N. and Hanke, D. E. (1985) The control of bud dormancy in potato tubers. Evidence for the primary role of cytokinins and a seasonal pattern of changing sensitivity to cytokinins. Planta **165**, 359–365
19 Hartmann, A., Senning, M., Hedden, P., Sonnewald, U. and Sonnewald, S. (2011) Reactivation of meristem activity and sprout growth in potato tubers require both cytokinin and gibberellin. Plant Physiol. **155**, 776–796
20 Rohde, A. and Bhalerao, R. P. (2007) Plant dormancy in the perennial context. Trends Plant Sci. **12**, 217–223
21 Turnbull, C. G. N. and Hanke, D. E. (1985) The control of bud dormancy in potato tubers. Measurement of the seasonal pattern of changing concentrations of zeatin-cytokinins. Planta **165**, 366–376
22 Scatchard, G. (1949) The attractions of proteins for small molecules and ions. Ann. N.Y. Acad. Sci. **51**, 660–672
23 Tamura, K., Peterson, D., Peterson, N., Stecher, G., Nei, M. and Kumar, S. (2011) MEGA5: molecular evolutionary genetics analysis using maximum likelihood, evolutionary distance, and maximum parsimony methods. Mol. Biol. Evol. **28**, 2731–2739
24 Saitou, N. and Nei, M. (1987) The neighbor-joining method: a new method for reconstructing phylogenetic trees. Mol. Biol. Evol. **4**, 406–425
25 Fesenstein, J. (1985) Confidence limits on phylogenies: an approach using the bootstrap. Evolution **39**, 783–791
26 Zuckerkandl, E. and Pauling, L. (1965) Evolutionary divergence and convergence in proteins. In Evolving Genes and Proteins (Bryson, V. and Vogel, H. J., eds), pp. 97–166, Academic Press, New York
27 Chaudhary, K., Ting, L. M., Kim, K. and Roos, D. S. (2006) *Toxoplasma gondii* purine nucleoside phosphorylase biochemical characterisation, inhibitor profiles, and comparision with the *Plasmodium falciparum* ortholog. J. Biol. Chem. **281**, 25652–25658
28 Kicska, G. A., Tyler, P. C., Evans, G. B., Furneaux, R. H., Kim, K. and Schramm, V. L. (2002) Purine-less death in *Plasmodium falciparum* induced by immucillin-H, a transition state analogue of purine nucleoside phosphorylase. J. Biol. Chem. **277**, 3219–3225
29 Moshides, J. S. (1988) Enzymatic determination of the free cholesterol fraction of high-density lipoprotein in plasma with use of 2,4,6-tribromo-3-hydroxybenzoic acid. Clin. Chem. **34**, 1799–1804
30 Foo, E., Morris, S. E., Parmenter, K., Young, N., Wang, H., Jones, A., Rameau, C., Turnbull, C. G. and Beveridge, C. A. (2007) Feedback regulation of xylem cytokinin content is conserved in pea and *Arabidopsis*. Plant Physiol. **143**, 1418–1428
31 Hellens, R. P., Edwards, A., Leyland, N. R., Bean, S. and Mullineaux, P. M. (2000) pGreen: a versatile and flexible binary Ti vector for *Agrobacterium*-mediated plant transformation. Plant Mol. Biol. **42**, 819–832
32 Visser, R. G. F. (1991) Regeneration and transformation of potato by *Agrobacterium tumefaciens*. In Plant Tissue Culture Manual: Fundamentals And Applications, Vol B5 (Lindsey, K., ed.), pp. 1–9, Kluwer Academic Publishers, Dordrecht
33 Jones, L, Hamilton, A. J., Voinnet, O., Thomas, C. B., Maule, A. J. and Baulcombe, D. C. (1999) RNA-DNA interactions and DNA methylation in post-transcriptional gene silencing. Plant Cell **11**, 2291–2301
34 Lu, R., Malcuit, I., Moffett, P., Ruiz, M. T., Peart, J., Wu, A.-J., Pathjen, J. P., Bendahmane, A., Day, L. and Baulcombe, D. C. (2003) High throughput virus-induced gene silencing implicates heat shock protein 90 in plant disease resistance. EMBO J. **22**, 5690–5699

35 Faivre-Rampant, O., Gilroy, E. M., Hrubikova, K., Hein, I., Millam, S., Loake, G. J., Birch, P., Taylor, M. and Lacomme, C. (2004) Potato virus X-induced gene silencing in leaves and tubers of potato. Plant Physiol. **134**, 1308–1316
36 Lewsey, M., Robertson, F. C., Canto, T., Palukaitis, P. and Carr, J. P. (2007) Selective targeting of miRNA-regulated plant development by a viral counter-silencing protein. Plant J. **50**, 240–252
37 Gopal, J., Minocha, J. L. and Dhaliwal, H. S. (1998) Microtuberisation in potato (*Solanum tuberosum* L.). Plant Cell Rep. **10**, 794–798
38 Nakai, K. and Horton, P. (1999) PSORT: a program for detecting sorting signals in proteins and predicting their subcellular localisation. Trends Biochem. Sci. **24**, 34–36
39 Mushegian, A. R. and Koonin, E. V. (1994) Unexpected sequence similarity between nucleosidases and phosphoribosyltransferases of different specificity. Protein Sci. **3**, 1081–1088
40 Ealick, S. E., Rule, S. A., Carter, D. C., Greenhough, T. J., Babu, Y. S., Cook, W. J., Habash, J., Helliwell, J. R., Stoeckler, J. D. and Parks, Jr, R. E. (1990) Three-dimensional structure of human erythrocytic purine nucleoside phosphorylase at 3.2Å resolution. J. Biol. Chem. **265**, 1812–1820

Received 14 June 2013/3 December 2013; accepted 10 December 2013
Published as BJ Immediate Publication 10 December 2013, doi:10.1042/BJ20130792

41 Prinsen, E., Redig, P., Vandongen, W., Esmans, E. L. and Vanonckelen, H. A. (1995) Quantitative analysis of cytokinins by electrospray tandem mass spectrometry. Rapid Commun. Mass Spectrom. **9**, 948–953
42 Chen, C. M. (1997) Cytokinin biosynthesis and interconversion. Physiol. Plant. **101**, 665–673
43 Michaelis, L. and Menten, M. L. (1913) Die kinetik der invertinwirkung. Biochemische Zeitschrift **49**, 333–369
44 Matsubara, S., Shiojiri, S., Fujii, T., Ogawa, N., Imamura, K., Yamagishi, K. and Koshimizu, K. (1977) Synthesis and cytokinin activity of (R)-(+)- and (S)-(−)-dihydrozeatins and their ribosides. Phytochemistry **16**, 933–937
45 Burch, L. R. and Stuchbury, T. (1987) Activity and distribution of enzymes that interconvert purine bases, ribosides and ribotides in the tomato plant and possible implications for cytokinin metabolism. Physiol. Plant. **69**, 283–288
46 Doree, M. and Terrine, C. (1973) Enzymatic synthesis of ribonucleoside-5′-phosphates from some N^6-substituted adenosines. Phytochemistry **12**, 1017–1023
47 Cornish-Bowden, A. (1979) Two-substrate reactions. In Fundamentals of Enzyme Kinetics, First edition, pp. 99–129, Butterworths, London

Biochem. J. (2014) **458**, 225–237 (Printed in Great Britain) doi:10.1042/BJ20130792

online data

SUPPLEMENTARY ONLINE DATA

A purine nucleoside phosphorylase in *Solanum tuberosum* L. (potato) with specificity for cytokinins contributes to the duration of tuber endodormancy

Jennifer R. BROMLEY*[1], Barbara J. WARNES*, Christine A. NEWELL*, Jamie C. P. THOMSON*[2], Celia M. JAMES*, Colin G. N. TURNBULL† and David E. HANKE*[3]

*Department of Plant Sciences, University of Cambridge, Downing Street, Cambridge CB2 3EA, U.K.
†Department of Life Sciences, Imperial College London, London SW7 2AZ, U.K.

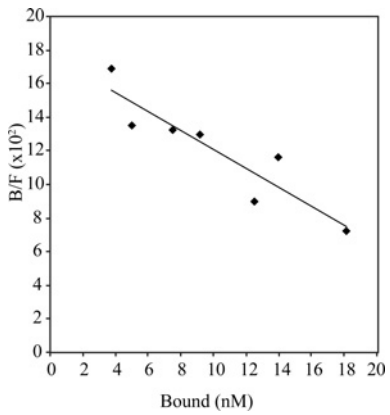

Figure S1 Scatchard analysis of ZR-[^{3}H]diol binding by partially purified potato stolon tip protein (50–75 % ammonium sulfate 'cut')

Each point is the mean of results from duplicate experiments. B, bound fraction; F, free fraction.

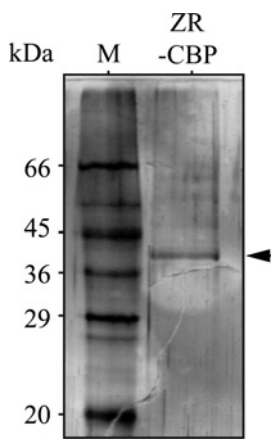

Figure S2 SDS/PAGE analysis of CK-binding proteins purified by affinity chromatography from IT stage potato stolon tips

ZR–CBP, the biotinylated ZR–CK binding protein complex eluted from the affinity column. The sizes of the molecular mass markers (M) are shown in kDa. The arrow indicates the position of the major protein which yielded the partial amino acid sequence of StCKP1.

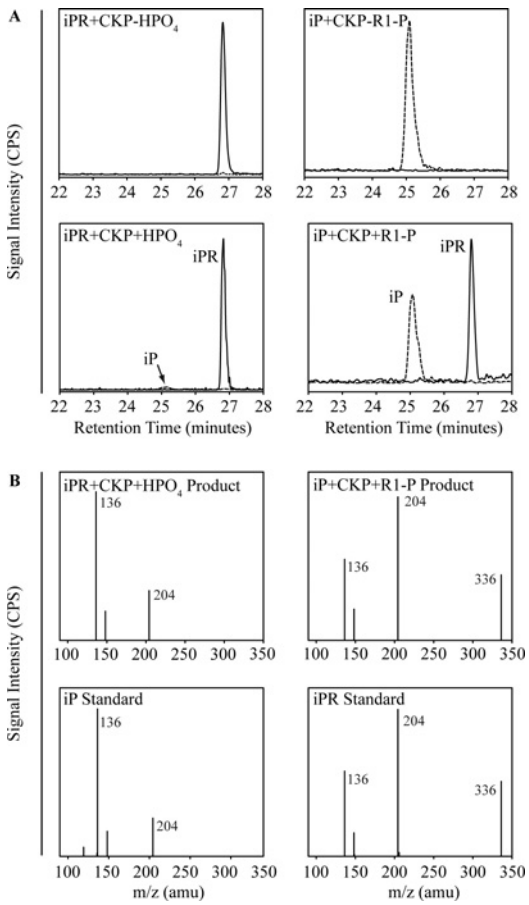

Figure S3 Phosphorylase activity of recombinant StCKP1, in the synthetic and phosphorolytic directions, on iP and iPR substrates

LC-MS/MS analysis of products of purified recombinant StCKP1 activity on iP and iPR in the presence of R1-P and P_i (HPO_4) respectively. Reactions were terminated after 5 min. (**A**) EPI MS/MS full-scan total ion chromatograms. Broken lines represent data collected in the iP channel (MS/MS products of *m/z* 204) and continuous lines in the iPR channel (MS/MS products of *m/z* 336). (**B**) MS/MS spectra confirming identity of reaction product peaks from (**A**) and corresponding authentic standards. The left-hand panel shows iP spectra (retention time 25.15 min) and the right-hand panel shows iPR spectra (26.81 min). iP + CKP + R1-P, iP plus R1-P and protein; iP + CKP-R1P, iP plus protein, no-R1-P control; iPR + CKP + HPO_4, iPR plus P_i and protein; iPR + CKP-HPO_4, iPR plus protein, no-P_i control. amu, atomic mass unit.

[1] Current address: Feedstocks Division, Joint BioEnergy Institute, Emeryville, CA 94608, U.S.A., and Physical Biosciences Division, Lawrence Berkeley National Laboratory, Berkeley, CA 94720, U.S.A.
[2] Current address: Pfizer Inc, Eastern Point Road, Groton, CT 06340, U.S.A.
[3] To whom correspondence should be addressed (email deh1000@cam.ac.uk).

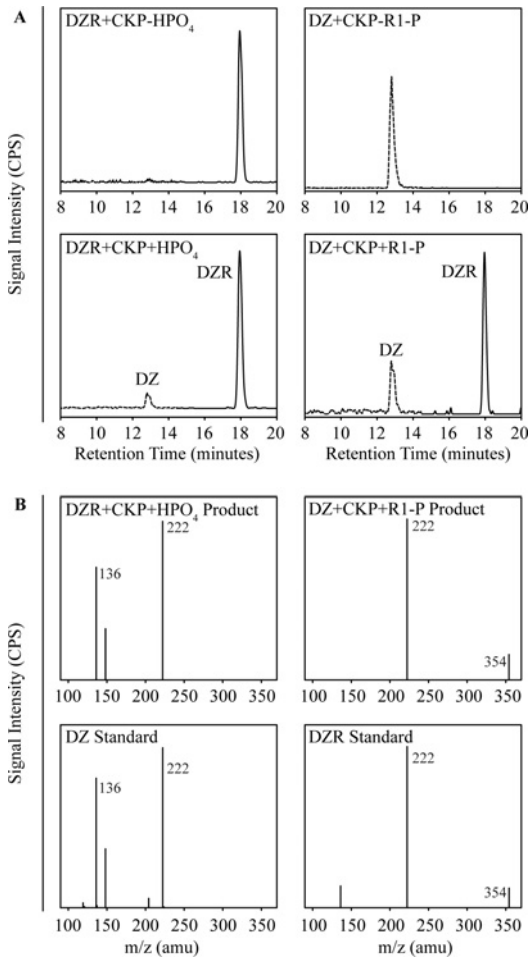

Figure S4 Phosphorylase activity of StCKP1, in the synthetic and phosphorolytic directions, on DZ and DZR substrates

LC-MS/MS analysis of products of purified recombinant StCKP1 activity on DZ and DZR in the presence of R1-P and P_i (HPO_4) respectively. Reactions were terminated after 5 min. (**A**) EPI full-scan MS/MS total ion chromatograms. Broken lines represent data collected in the DZ channel (MS/MS products of *m/z* 222) and continuous lines in the DZR channel (MS/MS products of *m/z* 354). (**B**) MS/MS spectra confirming identity of reaction product peaks from (**A**) and corresponding authentic standards. The left-hand panel shows DZ spectra (retention time 12.79 min) and the right-hand panel shows DZR spectra (17.96 min). DZ + CKP + R1-P, DZ plus R1-P and protein; DZ + CKP-R1P, DZ plus protein, no-R1-P control, DZR + CKP + HPO_4, DZR plus P_i and protein; DZR + CKP-HPO_4, DZR plus protein, no-P_i control. amu, atomic mass unit.

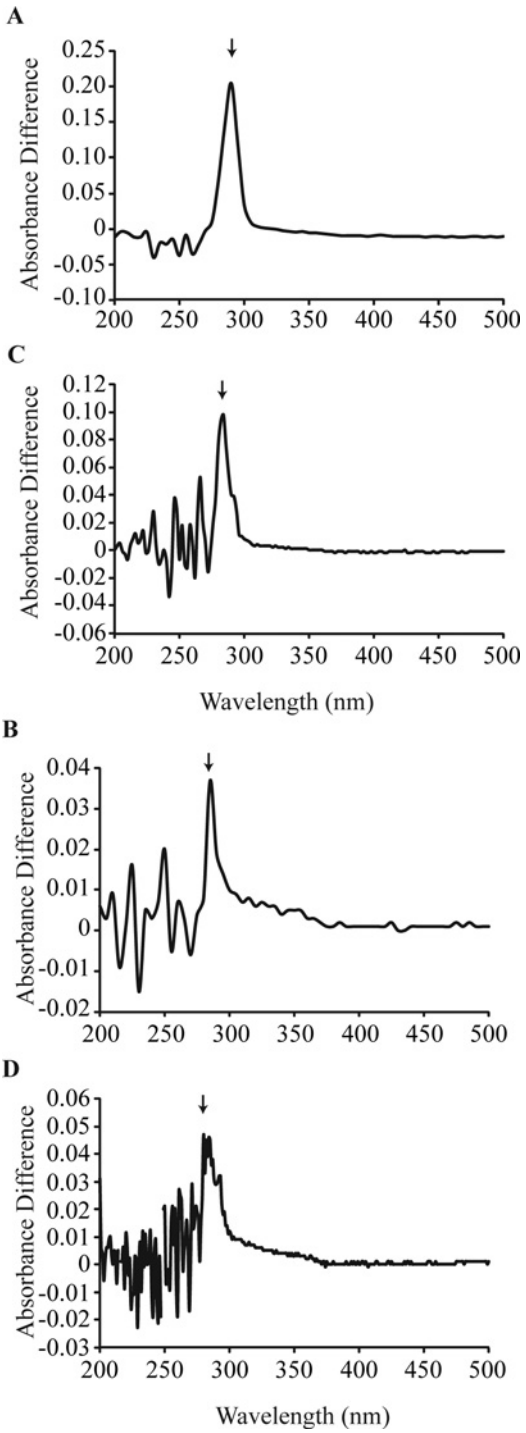

Figure S5 Difference in absorbance between the base and riboside forms of CKs and Ade

Arrows mark the peak absorbance difference (285 nm) as used for monitoring the formation of riboside. (**A**) iP minus iPR; (**B**) Z minus ZR; (**C**) DZ minus DZR; (**D**) Ade minus Ado.

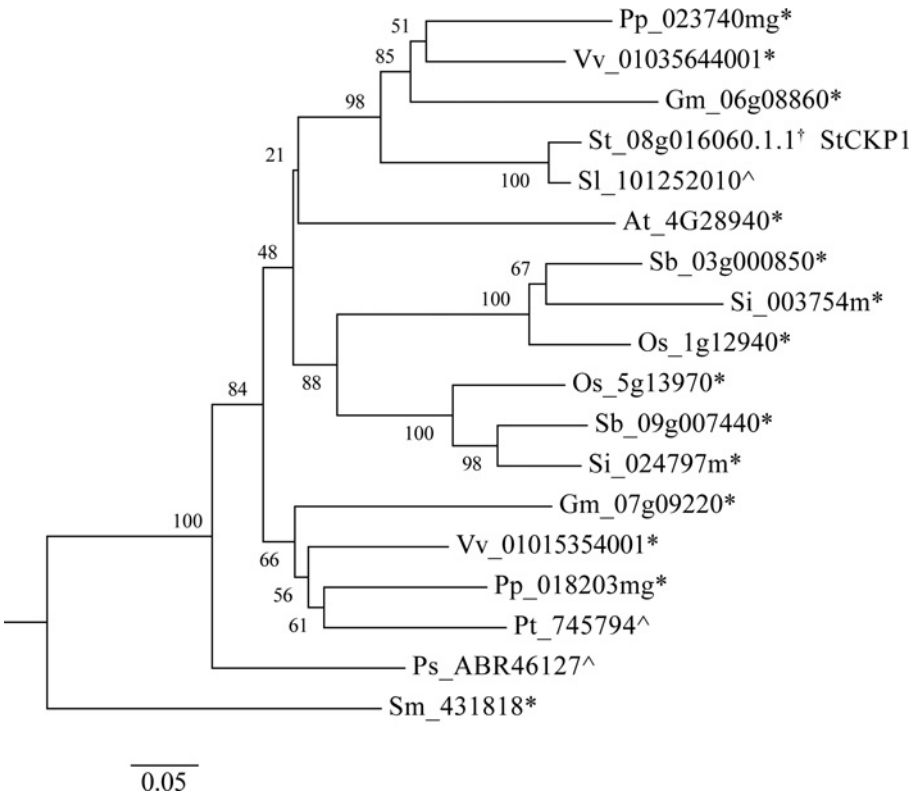

Figure S6 Phylogenetic analysis of CKP-like proteins

The optimal tree with the sum branch length of 2.92 is shown. The percentage of replicate trees in which the associated taxa clustered together in the bootstrap test is shown next to the branches. The tree is drawn to scale, with branch lengths in the same units as those of the evolutionary distances used to infer the tree. Lower plants are represented by *Selaginella moellendorffii* (Sm), gymnosperms by *Picea sitchensis* (Ps), monocotyledonous angiosperms by *Setaria italica* (Si), *Oryza sativa* (Os) and *Sorghum bicolor* (Sb), whereas dicotyledonous angiosperms are represented by *Populus trichocarpa* (Pt), *Glycine max* (Gm), *Prunus persica* (Pp), *S. tuberosum* (St), *Vitis vinifera* (Vv), *Solanum lycopersicum* (*Sl*) and *A. thaliana* (At). * denotes gene identifiers from Phytozome, ^ from NCBI and † from Spud DB.

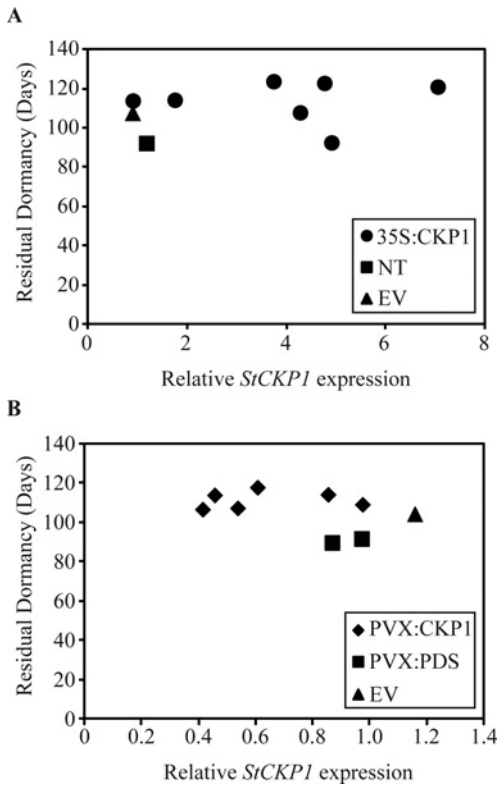

Figure S7 Duration of residual dormancy when *StCKP1* was (A) up-regulated by overexpression under the 35S promoter ($r^2 = 0.305$) and (B) down-regulated by VIGS ($r^2 = -0.248$)

Data points represent mean dormancy for 15 tubers, between 5 and 40 g of FM, harvested from a single plant. Each individual plant represents a separate transformation or infection event. *StCKP1* expression was normalized to non-transformed controls for overexpressing lines (NT = 1.0) and normalized to empty vector controls for VIGS lines (EV = 1.0).

Received 14 June 2013/3 December 2013; accepted 10 December 2013
Published as BJ Immediate Publication 10 December 2013, doi:10.1042/BJ20130792

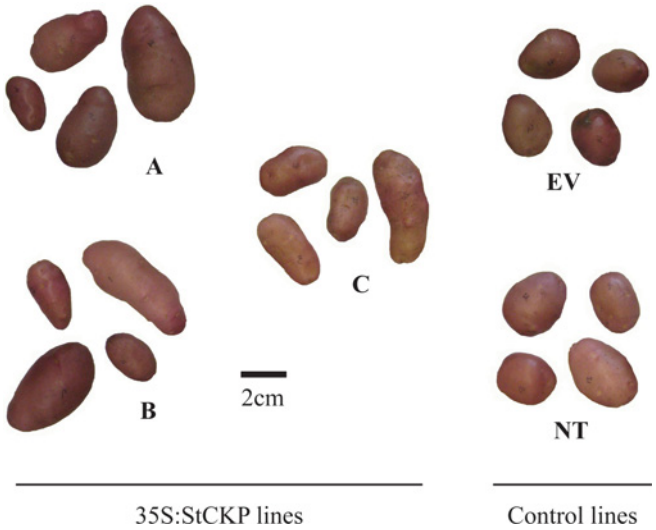

Figure S8 Representative tubers from plants overexpressing *StCKP1*

The lines shown correspond to three lines shown in Figures 7(B) and 7(C) of the main text. Plants were grown in 40-cm-diameter pots in growth chambers at 21 °C, 16 h light/8 h dark, 200 μmol · m^{2} · s^{-1} photosynthetically active radiation and 65 % humidity. EV, empty vector transgenic control; NT, non-transformed.